

Article

# Development of Polylactic Acid Films with Selenium Microparticles and Its Application for Food Packaging

Rui Lu <sup>1</sup>, Dur E. Sameen <sup>1</sup>, Wen Qin <sup>1</sup>, Dingtao Wu <sup>1</sup>, Jianwu Dai <sup>2</sup>, Suqing Li <sup>1,\*</sup> and Yaowen Liu <sup>1,3,\*</sup>

<sup>1</sup> College of Food Science, Sichuan Agricultural University, Yaan 625014, China; lr548624lr@163.com (R.L.); sameen388@yahoo.com (D.E.S.); Qinwen@sicau.edu.cn (W.Q.); wudingtao@yeah.net (D.W.)

<sup>2</sup> College of Mechanical and Electrical Engineering, Sichuan Agricultural University, Ya'an 625014, China; daijianwu@126.com

<sup>3</sup> California NanoSystems Institute, University of California, Los Angeles, CA 90095, USA

\* Correspondence: lsq03\_2001@163.com (S.L.); lyw@my.swjtu.edu.cn (Y.L.)

Received: 13 February 2020; Accepted: 14 March 2020; Published: 18 March 2020



**Abstract:** Selenium is a natural element which exists in the human body and plays an important role in metabolism. Along with this, selenium also possesses antibacterial and antioxidant properties. Using selenium microparticles (SeMPs) in food packaging films is exceptional. In this experiment, a solution casting method was used to make film. For this purpose, we used polylactic acid (PLA) as a substrate for the formation of a film membrane while SeMPs were added with certain ratios to attain antibacterial and antioxidant properties. The effects of SeMPs on the PLA film and the value of SeMPs in food packaging film production were investigated. The effects of the SeMPs contents on the features of the film, such as its mechanical property, solubility, swelling capacity, water vapor permeability, antioxidant activity, and the antibacterial activity of the composite membrane against *Staphylococcus aureus* (Gram-positive) and *Escherichia coli* (Gram-negative) strains, were studied. The results manifest that the PLA/SeMPs films showed higher water resistance, UV resistance, antioxidant activity, and antibacterial activity than pure PLA film. When the concentration of SeMPs was 1.5 wt%, the composite membrane showed the best comprehensive performance. Although the tensile strength and elongation at break of the membrane were slightly reduced by the addition of SeMPs, the results show that PLA/SeMPs films are still suitable for food packaging and would be a very promising material for food packaging.

**Keywords:** PLA; SeMPs; antibacterial films; casting method

## 1. Introduction

In recent years, due to environmental protection and the sustainability of renewable resources, the demand for biodegradable packaging is rising [1,2]. Plastics are multifaceted materials that are extensively used in food packaging as well as in non-food items. Polylactic acid (PLA) is a new material derived from corn, sugar beets, potato starch or other plants that can regenerate [3,4]. Many studies have shown that it is biodegradable into CO<sub>2</sub>, H<sub>2</sub>O and other small molecules in composting conditions [5]. In addition, it also has many excellent properties, such as strong applicability, low cost, good biocompatibility, optical clarity, biodegradability, good processing properties, thermoplasticity and excellent mechanical properties [6,7]. Due to these excellent performances, PLA is not only used in packaging but also used in various products like cups, bathtubs, packaging films, pallets and other products [8,9]. The Food and Drug Administration (FDA) also recognizes PLA as GRAS (generally recognized as safe), such that it can encounter food [10]. It is one of the most promising polymeric materials with high application value [11].

An important reason behind the need for food packaging with antibacterial properties is the ever-growing issue of increasing foodborne microorganisms, which necessitates higher requirements for the functionality of food packaging that ensures the retention of the food quality [12]. The PLA membrane has no antimicrobial property. The incorporation of nanomaterials (nano-metals, nano-cellulose, nano-clay and so on) improves the properties and helps to obtain antibacterial activity, prevent ultraviolet radiation and other additional functional properties [13]. In this regard, metal nanoparticles such as those of titanium, silver, and zinc have been found to improve the antimicrobial activity of biodegradable polymer films [14–16]. Some studies have shown the successful incorporation of nanoparticles in the PLA films to enhance the properties of films. Athanasoulia et al. [17] made the TiO<sub>2</sub>/PLA membrane by extrusion melt blending and investigated the influence of the incorporation of TiO<sub>2</sub> nano particles on the performance and features of a brittle crystalline poly-matrix. They found that a 20/80 *w/w* TiO<sub>2</sub>/PLA nanocomposite offered favorable bacteriostatic effects both under UV light and in the dark. Shebi et al. [18] prepared the honeycomb membrane by using the breath figure method. This study explained that the nanomaterials (H-PLA/GST) showed obvious bacteriostatic properties to *S. aureus*, both in visible light and in dark conditions. Munteanu et al. [19] used the electrostatic spinning method to mix polylactic acid (PLA), silver nanoparticles (AgNPs) and Vitamin E, and prepared the PLA/AgNPs/Vitamin E nanometer fiber membrane. This study showed that the growth inhibition rate of the nanofibers against *E. coli*, *Listeria monocytogenes* and *Salmonella typhimurium* was up to 100%. Shameli et al. [20] reacted AgNPs with PLA by the chemical reduction method in diphasic solvent. The antibacterial properties of the Ag/PLA-NC membranes were studied, and the results show that with the increase in the AgNPs ratio, the antibacterial properties against *E. coli* and *S. aureus* were enhanced. Like these commonly used materials, SeMPs also present potential for similar applications [21–24].

Selenium is necessary for the survival of mammals; it is a very important dietary trace element. Many researches have shown that selenium has a wide range of pharmacological effects as well as important physiological functions [25,26]. SeMPs are widely regarded as potential heart protective and therapeutic agents because of their remarkable antioxidant and disease-preventing properties [27,28]. Nanometer selenium of about 5 to 550 nm in size is naturally found in the human body [29]. A lack of selenium can modify bone metabolism and retards growth and augment the danger of bone disease [30–32], but elemental selenium also has some toxicity [33,34]. SeNPs have been shown to have the same efficacy and bioavailability as other types of selenium, but have a reduced risk of selenium poisoning [35,36]. SeNPs have also been noted to play a part in the modulation of immune responses [37] and maintenance of bone health [38]. However, SeMPs have not been well developed and applied.

In short, the main purpose of this experiment is to prepare a PLA/SeMP composite membrane by the solution casting method, and then use various analytical techniques to characterize its performance in order to analyze the application value of this material in the field of food packaging. This study also verifies whether SeMPs have antibacterial or antioxidant functions like other nanomaterials, in order to strengthen the polymer matrix composite membrane.

## 2. Materials and Methods

### 2.1. Materials

PLA particles (weight-average molecular weight: 100,000) were purchased from Shenzhen Esun Industrial Co., Ltd. (Shenzhen, China). SeMPs (average particle size: 900 nm) were purchased from Zibo Lanjing Nanomaterials Co., Ltd (Shandong, China), and Span-80 was provided by Chengdu Kelong Reagent Co., Ltd (Chengdu, China). Meanwhile, all other chemical reagents and solvents were purchased from Chengdu Kelong Reagent Co., Ltd (Chengdu, China).

## 2.2. Preparation of PLA and PLA/SeMPs Composite Membranes

The solvent casting method was used for the preparation of all membranes (Figure 1); the concentration range of SeMPs was determined by preliminary experiments. First, 2 g of PLA was added to 20 g of chloroform at room temperature and kept under vigorous stirring with a stirrer until the PLA was completely dissolved, and thus a 10% (*w/w*) PLA solution was prepared. Span-80 was added to the solution with a mass fraction of 2% as a plasticizer. The solution was then poured onto a clean and flat glass plate (12 × 12 cm<sup>2</sup>). The glass plate containing the solution was put into the oven and dried at 50 °C to prepare pure PLA membranes. SeMPs (0.1 g; 0.2 g; 0.3 g; 0.4 g) were added up to the mixed solution (10% PLA and 2% Span-80) and stirred intensely for 20 min, after which the PLA/SeMPs membrane solution was obtained. The solutions of different proportions were poured on the glass plate and dried at 50 °C until the solvent completely evaporated to prepare composite membranes (Table 1), which were then stored in dry conditions until use for further testing.

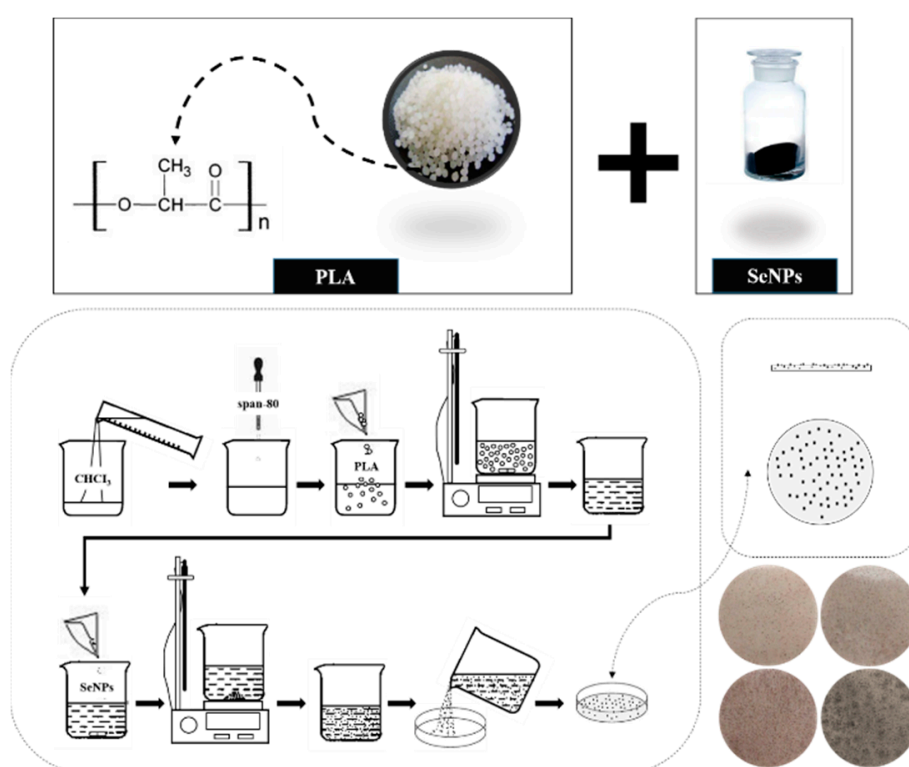


**Figure 1.** Preparation process of poly(lactic acid) (PLA) and PLA/SeMPs composite films.

**Table 1.** Sample codes and composition for the PLA/SeMPs film-forming solutions.

Sample	SeMPs (g)	PLA (g)	Span-80 (g)
PLA	0	20	4
PLA/SeMPs-0.5%	1	20	4
PLA/SeMPs-1%	2	20	4
PLA/SeMPs-1.5%	3	20	4
PLA/SeMPs-2%	4	20	4

## 2.3. Morphology Studies

The morphological analysis of PLA and PLA/SeMPs composite membranes was done by scanning electron microscopy (SEM; JSM-639OLV, JEOL, Tokyo, Japan) and transmission electron microscopy (TEM; 2100 microscope, JEOL, Tokyo, Japan). For SEM analysis, the sample was coated with the gold particles through the physical vapor deposition (PVD) technique. The coating was done by Baltec SCD

005 sputter coater, using a 30-mA current from 50 mm distance for 180 s. The sample was prepared by placing drops of suspension containing particles on the carbon films which are supported by 300-mesh grid of copper for the transmission electron microscope (TEM) analysis.

#### 2.4. Fourier-Transform Infrared Experiment (FTIR)

The attenuated total reflectance Fourier transform infrared (which is denoted by the abbreviation (ATR-FTIR)) spectrometry technique was used to study the chemical structure of the PLA and PLA/SeMPs composite membranes and to observe possible interactions between PLA and SeMPs. The specimens were cut into small sections, each for different composite membranes, and they were analyzed in resolution at  $4\text{ cm}^{-1}$ . The velocity for scanner was 2.2 kHz, the aperture setting was set as 6 mm, the scan time was 32 s for the background, the scan time for the sample was 32 s, the total scans per sample were 100, and the range was  $400\text{--}4000\text{ cm}^{-1}$ . The spectral output was recorded in the absorption mode, as a function of the wavenumber, a Bruker 66 spectrometer (Jena, Germany) was used.

#### 2.5. Density Test

The flat and smooth composite membranes were cut into samples with area  $s$ . The mass of each sample was measured with electronic scales with an accuracy of 0.1 mg, denoted as  $m$ . The thickness of the samples was measured with a thickness gauge. We measured the thickness from one center point and four surrounding points of the sample, and then recorded the average thickness  $d$ , with an accuracy of  $1\text{ }\mu\text{m}$ . The above steps were repeated three times for each membrane sample and the average value was used. The membrane density ' $\rho$ ' was computed according to the following formula [39]:

$$\rho = \frac{m}{s \times d}$$

#### 2.6. Mechanical Property Analysis

Each film was cut into rectangles 100 mm in length and 10 mm in width. A universal testing machine (UTM, Instron 5583, Norwood, MA, USA) was used for tensile strength tests with crosshead speeds of 250 mm/min and an 80 mm gauge length. Each film was tested five times, and the average value was recorded for subsequent analysis [40].

#### 2.7. Swelling Capacity and Solubility of PLA/SeMP Composite Membranes

The swelling capacity and solubility of the PLA and PLA/SeMP composite membranes were tested using the method exploited by Gontard et al. [41]. The membranes were cut into rectangles 40 mm in length and 10 mm in width, and then weighed, denoted as the initial weight  $m_1$  of the film. The rectangular sample was immersed in distilled water (50 mL) for 24 h, and allowed to settle at room temperature. Then, we removed the samples from the water, drained the surface carefully with filter paper and then weighed the samples. We repeated these steps until we obtained a constant weight, which was recorded as  $m_2$ . Then, the samples were placed in an oven at  $100^\circ\text{C}$  to dry, until the weight stabilized, and the weight was recorded as  $m_3$ . Each value was the average of three samples for parallel experiments. The following formula was used for the calculation of swelling capacity and solubility:

$$\text{Swelling capacity} = \frac{m_2 - m_1}{m_1} \times 100\%$$

$$\text{Solubility} = \frac{m_1 - m_3}{m_1} \times 100\%$$

where  $m_1$  (g) is the initial weight of a rectangular sample,  $m_2$  (g) refers the weight of the rectangular sample after water absorption, and  $m_3$  (g) represents the weight of the rectangular sample after drying.

## 2.8. Permeability Experiments

Referring to the method reported previously by Fabra et al. [42], we first fixed the samples then placed the silica gel in a drying tower (with a temperature of 25 °C, with a relative humidity of 0%). The control sample was a cup covered with aluminum foil to estimate the solvent loss during the sealing. Once the stable state was obtained, the analytical balance (accuracy 0.0001 g) was used for weighing the cup every 2 h. The slope of steady-state permeability with time in the weight loss curve was used to calculate the water vapor permeability coefficient. The mass loss was obtained by subtracting the loss through sealing from the total mass loss. Finally, the thickness of the samples was measured to calculate the water vapor permeability. Each value was the average of three samples for parallel experiments.

## 2.9. Color Measurements

The color parameters of the composite membranes were measured by a CR-400 Chroma-Meter (Konica Minolta, Barcelona, Spain) [43]. A composite membrane was placed on the surface of a white standard plate (calibration plate values:  $L^* = 88.04$ ,  $a^* = 0.72$ , and  $b^* = -4.34$ ). Color parameter measurement used the CIELAB color scale:  $L^* = 0$  (black) to  $L^* = 100$  (white),  $-a^*$  (greenness) to  $+a^*$  (redness),  $-b^*$  (blueness) to  $+b^*$  (yellowness), and the  $\Delta E^*$  (color difference) was calculated as:

$$\Delta E^* = \sqrt{\left(L^*_{control} - L^*_{sample}\right)^2 + \left(a^*_{control} - a^*_{sample}\right)^2 + \left(b^*_{control} - b^*_{sample}\right)^2}$$

where the white standard plate was the control sample. Each sample was measured 10 times.

## 2.10. DPPH Free Radical Scavenging Activity

The antioxidant activity of the PLA and PLA/SeMP composite membranes was evaluated by assaying the DPPH free radical scavenging [44], with a slight modification. All composite membranes were cut into 20 mm × 20 mm size samples, which were placed in a beaker filled with 50 mL of absolute ethyl alcohol, and then mixed until complete dissolution. The DPPH solution was prepared by mixing 1 mL of membrane solution with 4 mL of absolute ethyl alcohol of DPPH ( $75 \times 10^{-3}$  mol/L). The DPPH solution was kept in the dark for 30 min at room temperature. The UV absorbance of the determination of DPPH solution was determined at 517 nm. The following formula was used to calculate the DPPH scavenging activity:

$$\text{DPPH scavenging activity(\%)} = \frac{A_{DPPH} - A_s}{A_{DPPH}} \times 100\%$$

where  $A_{DPPH}$  is the UV absorbance of the absolute ethyl alcohol solution of DPPH at 517 nm and  $A_s$  is the UV absorbance of the determination of DPPH solution at 517 nm. Detections were tested three times for each sample, and the average values were considered.

## 2.11. Light Transmittance

The composite membranes with smooth surface and no mechanical damage were selected to measure the light transmittance. Measurements were performed using the method developed by Yu et al. [45]. The composite membrane was cut into rectangles 10 mm in width and 40 mm in length. Then, the rectangular specimens were placed tightly on the inner wall of a 10-mm colorimetric ware for light transmittance measurements (600 nm using a UV–visible spectrophotometer). Blank colorimetric ware was used as a control. Each value used for analysis was the average of three parallel experiments.

### 2.12. Seal strength Determination

Referring to ASTM Standard Method F88 for seal strength measurement of the composite membranes with slight modifications, the composite membranes were cut into strip samples 100 mm in length and 15 mm in width. A 10 mm heat-sealed area was sealed at 130 °C and 450 KPa for 3 s. The 2 unsealed edges of the sealed membranes were clamped separately to the universal testing machine (UTM, Instron 5583, Norwood, MA, USA) and held perpendicular to the test direction. A crosshead speed of 300 mm/min and a gauge length of 80 mm were used. Seal strength is the maximum force required to cause seal failure, expressed in N/m:

$$\text{Seal strength (N/m)} = \text{Peak force (N)} / \text{Film width(m)}$$

### 2.13. Antimicrobial Properties

The antimicrobial properties of the membranes were determined using the technique provided by Otoni et al. [46] with some modifications. *E. coli* and *S. aureus* (0.2 mL 10<sup>5</sup> CFU/mL) were inoculated in nutrient agar medium, respectively, and cultured for 24 h. Then, small disks 12 mm in diameter were cut from the samples (PLA and PLA/SeMP composite membrane, respectively) and were placed on the corresponding medium, cultured at 37 °C for 24 h. The inhibition zones were measured with a caliper, recorded in mm. All tests were performed in triplicate.

### 2.14. Statistical Analysis

All experiments tested multiple samples, and the final value was expressed as the mean ± standard deviation. SPSS software was used to conduct one-way analysis of variance (ANOVA). A value of  $p < 0.05$  was considered significant.

## 3. Results and Discussion

### 3.1. Morphology and Surface Characteristics of PLA/SeMPs Films

Figure 2a shows images of the composite films with different compositions, and Figure 2b shows the SEM micrographs of the corresponding films. The surfaces of the PLA present a continuous microstructure, which smooth and homogeneous, without holes or cracks. The PLA/SeMP composite membranes have no cracks, air bubbles, droplets and pores. Changes in the morphology of the PLA/SeMP membranes were significant compared to those noted for the PLA membranes. The surface of pure PLA was smooth and dense, while the surface of the PLA/SeMP membranes showed a slightly rough texture and the nanoparticles were distributed in the PLA matrix. The surface roughness arose from the SeMP molecules disrupting the compact structure of the PLA matrix. As the concentration of SeMP increased, the surface roughness of the membranes increased. As the SeMPs were dispersed in the chloroform solution for PLA dissolution without any surface treatment, the SeMPs appeared on the surface of the membrane. When the dosage was less than 1.5%, the distribution of nanoparticles was more uniform. Particle agglomeration occurred when the dosage of nanoparticles was increased further. Similar events have been reported in the previous literature [47]. To determine the morphology of SeMPs in the polymer, TEM was performed, and the microstructure images of the PLA/2% SeMP films are presented in Figure 2c. As seen in the figure, SeMPs were randomly distributed in the PLA matrix. At this concentration, the SeMPs began to agglomerate, corresponding to our intuitive assumption.

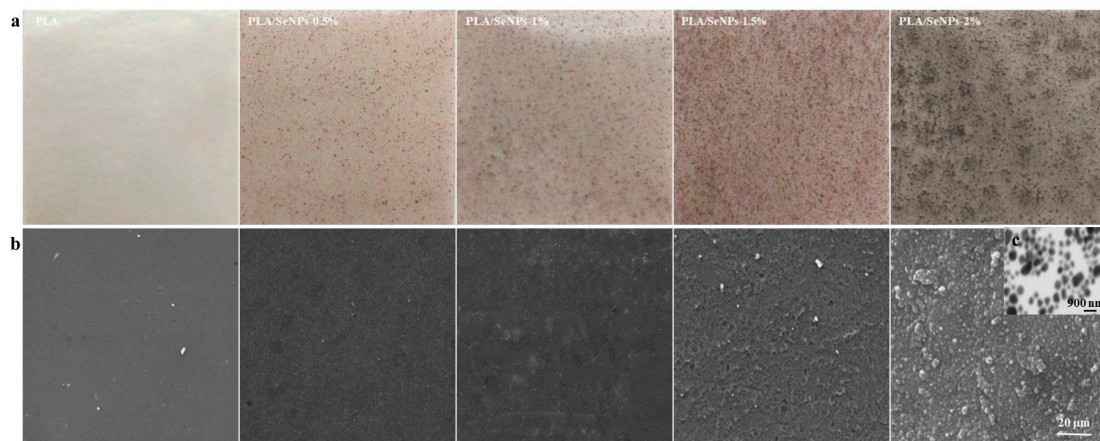


**Figure 2.** Physical characterization of PLA and PLA/SeMPs films. (a): Pictures of PLA and composite films with different concentrations; (b): scanning electron microscopy (SEM) images of the film samples corresponding to five films; (c): transmission electron microscopy TEM images of PLA/SeMPs-2% films.

### 3.2. Infrared Spectra

FTIR spectrum is an effective technique to research the interaction between functional groups based on the vibrational band shifts. Further characterization of the PLA and PLA/SeMP composite membranes was done by applying FTIR spectra. The band of PLA at  $2923\text{ cm}^{-1}$  represents the asymmetric stretching vibration of CH; the band at  $1747\text{ cm}^{-1}$  represents the stretching vibration of C=O; the band at  $1455\text{ cm}^{-1}$  is the bending vibration in the s-CH(CH<sub>3</sub>) plane; the peak value at  $1081\text{ cm}^{-1}$  stands for C–O stretching vibration and the peak values at  $870\text{ cm}^{-1}$  and  $753\text{ cm}^{-1}$  represent C–C stretching vibrations. Based on analysis of the spectra obtained for PLA, PLA/SeMPs, and SeMPs (Figure 3), the FTIR spectra of the membranes with or without nanoparticles showed similar general characteristics. There was no indication of chemical interactions between PLA and the SeMPs. No supplemental peak formation was observed, suggesting that no chemical bonds were formed between the PLA and SeMPs. This suggests that SeMPs were physically trapped within the polymer matrix, in agreement with the previously discussed results [48,49].

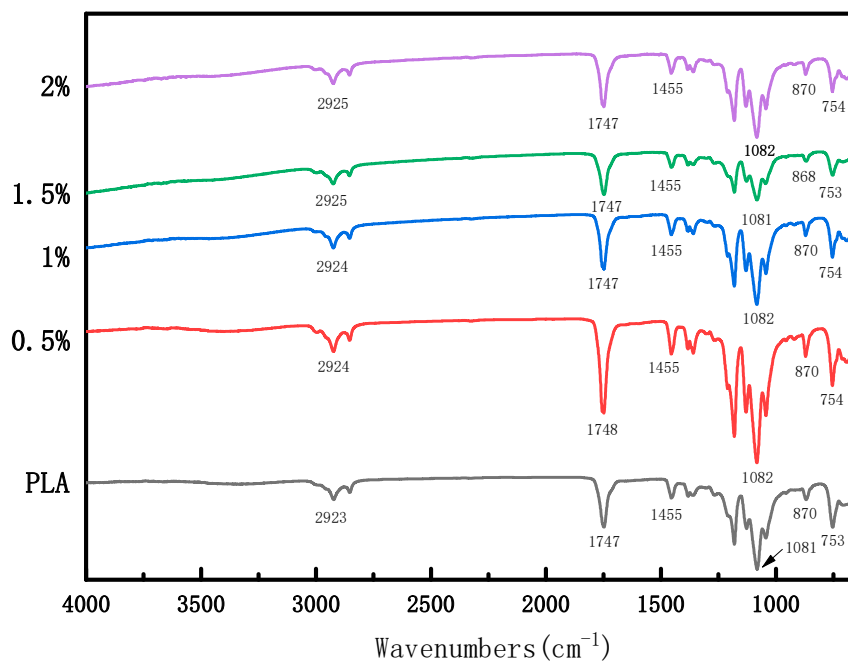


**Figure 3.** FTIR spectra of pure PLA and PLA/SeMPs membranes with different SeMPs weight ratios.

### 3.3. Density Tests

Table 2 lists the densities of the PLA and PLA/SeMP composite membranes. The density of the PLA was higher than all the composite membranes, which was  $1.14 \pm 0.09 \text{ g/cm}^3$ . Therefore, we can consider that the addition of SeMPs reduces the density of the PLA matrix. This may be due to the interactions between the two constituent materials and the violent agitation destroyed the original dense structure of the PLA matrix [39]. Moreover, on further addition of SeMPs, a trend of increase followed by a decrease was noted. The density increase may have been due to the increase in the solid content associated with SeMPs and the uniform distribution of SeMPs among PLA molecules [50]. When the concentration of SeMPs was so high that agglomeration occurred, the density decreased again [51]. When the mass fraction of SeMPs was 1.5%, the density reached the highest value for the composite membrane, at  $1.10 \pm 0.04 \text{ g/cm}^3$ —only 3.51% lower than that of the PLA film. As the mass score of SeMPs continues to increase to 2%, the density of the composite membrane suddenly decreased to a minimum of  $(0.91 \pm 0.02) \text{ g/cm}^3$ , which is 20.18% lower than that of the pure PLA.

**Table 2.** Physical properties and mechanical properties of PLA and PLA/SeMP composite membranes.

Sample	Thickness (mm)	Density ( $\text{g/cm}^3$ )	TS (MPa)	%E (%)
PLA	$0.08 \pm 0.01^a$	$1.14 \pm 0.09^a$	$23.34 \pm 1.81^a$	$272.16 \pm 33.61^a$
PLA/SeMPs-0.5%	$0.10 \pm 0.01^{ab}$	$0.99 \pm 0.08^{ab}$	$13.47 \pm 1.13^b$	$145.43 \pm 13.54^b$
PLA/SeMPs-1%	$0.11 \pm 0.01^{bc}$	$1.05 \pm 0.03^b$	$11.45 \pm 0.84^c$	$181.70 \pm 20.51^c$
PLA/SeMPs-1.5%	$0.13 \pm 0.02^c$	$1.10 \pm 0.04^c$	$9.28 \pm 0.52^d$	$111.64 \pm 18.11^{cd}$
PLA/SeMPs-2%	$0.17 \pm 0.03^d$	$0.91 \pm 0.02^c$	$6.89 \pm 0.39^e$	$96.70 \pm 15.64^e$

Notes: Letters of the same values are not statistically significant, according to Duncan's Multiple Range Test ( $p < 0.05$ ); a, b, and c, the means in the same column with the same letter are not significant different ( $p > 0.05$ ).

### 3.4. Tensile Properties

The membrane, which is used to keep food fresh, needs to remain intact under external pressure: therefore, excellent mechanical properties are essential [52]. Furthermore, elongation at break (%E) and tensile strength (TS) are major features in mechanical properties [53,54]. Table 2 shows the effects of adding different concentrations of SeMPs on the mechanical properties of the PLA membrane; the addition of SeMPs reduced the overall %E and TS for the membranes.

The TS of the composite film tended to worsen with an increase in the SeMPs content. When the mass fraction of SeMPs was 0.5%, the TS was  $13.45 \pm 1.13 \text{ MPa}$ . When the mass fraction of SeMPs was 2%, the TS of the film was the lowest, having decreased by 70.48% compared to that of the PLA membrane. The decrease in TS could be due to the high-speed magnetic agitation that caused some of the SeMPs to enter the PLA macromolecule chain during the film formation process in the composite film solution [55,56]. This damaged the original structure of the PLA, resulting in an increase in the brittleness and decrease in the binding force [57].

The lowering of %E on addition of additives and/or a filler to polymers is also a common trend observed in thermoplastic composites [58]. In this case, the %E of the PLA/SeMP composite film showed a tendency of first improvement and then deterioration. The trend noted for the %E might mainly be attributable to the particle shape [59]. When the mass fraction of SeMPs was 1%, the best %E of  $181.70\% \pm 20.51\%$  was noted. Then, the performance began to deteriorate, which might have been due to the aggregation of SeMPs [51].

Although the addition of SeMPs resulted in an overall decrease in the mechanical properties of the membrane, it still meets the requirements of food safety packaging [56]. The composite membrane with SeMPs content of 1% showed the best mechanical properties: its TS and %E were  $11.45 \pm 0.84 \text{ MPa}$  and  $181.70\% \pm 20.51\%$ , respectively.

### 3.5. Swelling Capacity and Solubility

The swelling capacity and solubility are very important factors for membranes, affecting their water resistance, especially in humid environments [49]. As shown in Figure 4, the PLA membranes were characterized by a higher swelling capacity than that of the PLA/SeMPs composite membranes. The addition of SeMPs significantly ( $p < 0.05$ ) reduced the swelling degree of the membrane in water. This may be because the SeMPs molecules entered the PLA molecules and blocked many gaps between the PLA molecules, so that water molecules could not enter these gaps and be adsorbed [60]. When the mass fraction of SeMPs was 2%, the swelling rate of the composite film was  $0.15 \pm 0.01\%$ , which was the lowest, and 94.81% lower than that of PLA membrane.

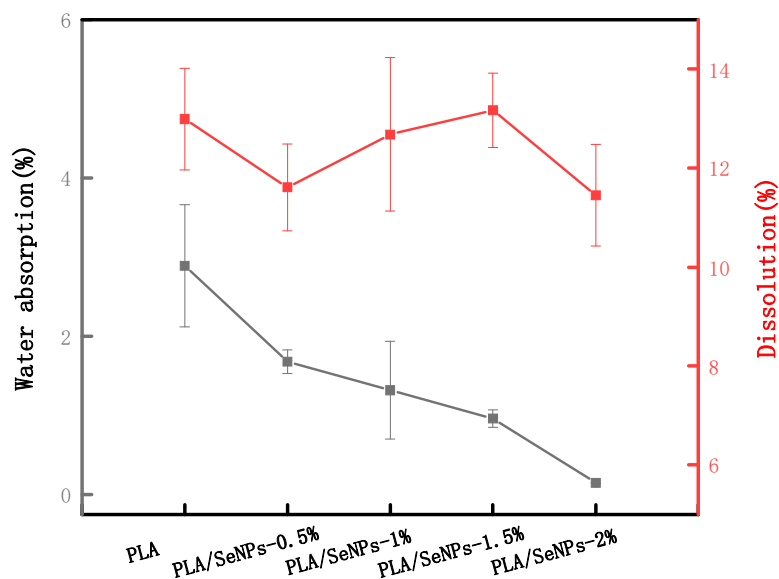


Figure 4. Water absorption and dissolution rate of different composite films.

No significant difference ( $p > 0.05$ ) was noted in the solubility of the composite membrane and pure PLA membrane with a change in the SeMP concentration. Since the overall swelling capacity and solubility of the membrane are very low, the material can be considered to protect the food in a humid environment.

### 3.6. Water Vapor Permeability

The water vapor permeability (WVP) reflects the ability of a film to prevent moisture transfer [61]. It is one of the important indices that help to evaluate the functions of edible membranes, which is influenced by numerous factors, such as the relative proportions of the ingredients in the formula, the thickness of the membrane, humidity and water activity [62]. A difference in the WVP of nanoparticle-containing films may be due to various factors, such as compatibility between the polymer matrix and the nanoparticles, the filler concentration, and the type of polymer used [63].

The WVP of the PLA and composite membranes is shown in Figure 5. The WVP of the pure PLA was  $5.12 \times 10^{-14}$  g·cm/cm<sup>2</sup>·s·Pa. The WVP first decreased at low SeMP concentrations (below 1.5%) and then increased with further addition of SeMPs. The WVP of the pure PLA was always higher than that of PLA/SeMP composite membranes. The PLA/1.5%-SeMP composite membrane showed the lowest WVP of  $3.55 \times 10^{-14}$  g·cm/cm<sup>2</sup>·s·Pa, which is 30.6% lower than that of the pure PLA. This may be due to the SeMPs entering the pores of the PLA molecular chain, resulting in the formation of a tortuous diffusion channel for the water vapor molecules in the polymer matrix [64]. This is like results obtained previously. Shankar et al. [65] reported that when AgNPs were mixed with PLA to prepare the composite membranes, the WVP value of the PLA/AgNPs membrane decreased.

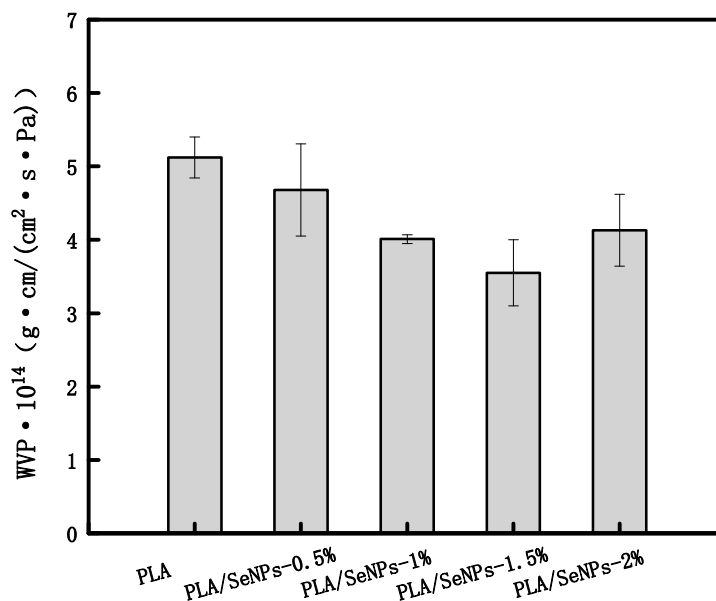


Figure 5. Water vapor permeability of different composite films. ( $p < 0.05$ ).

When the mass fraction of SeMPs was 2% (higher concentrations), the WVP of the composite membrane increased: it reached a value of  $4.13 \times 10^{-14}$  g·cm/cm<sup>2</sup>·s·Pa, which is only 19.34% lower than that of the pure PLA. It is likely because the nanofillers at high concentrations formed an agglomerated structure without homogeneous dispersion in the polymer matrix [2,66].

### 3.7. Color Measurements

Optical properties such as the color and gloss are related features, because they directly influencing the acceptance of the product by consumers [67,68]. Visually, both the PLA and PLA/SeMP membranes were transparent, although they darkened with the addition of SeMP. As noted in previous experiments, when the SeMP concentration reached 2%, agglomeration occurs, leading to this darkening. The effect of the SeMP concentration on the color of the films is shown in Table 3. As can be seen from the table, the addition of SeMP reduced the membrane lightness ( $L^*$ ) and resulted in membranes with a more bluish and reddish color, which are determined by the values of  $a^*$  and  $b^*$ , respectively. These changes lead to an increase in the total color difference ( $\Delta E^*$ ), compared to the SeMPs membranes. Similar changes in color parameters have been reported for chitosan-BSSCE films [69].

Table 3. Optical properties ( $L^*$ ,  $a^*$ ,  $b^*$ ,  $\Delta E^*$ ) of different composite films.

Sample	$L^*$	$a^*$	$b^*$	$\Delta E^*$
PLA	$85.91 \pm 0.21^a$	$-0.33 \pm 0.01^a$	$0.40 \pm 0.08^a$	$2.41 \pm 0.10^a$
PLA/SeMPs-0.5%	$82.84 \pm 0.23^b$	$-0.22 \pm 0.08^b$	$-0.70 \pm 0.09^b$	$6.12 \pm 0.23^b$
PLA/SeMPs-1%	$77.96 \pm 0.31^c$	$-0.13 \pm 0.03^c$	$-0.91 \pm 0.03^c$	$16.52 \pm 0.35^b$
PLA/SeMPs-1.5%	$71.81 \pm 0.54^d$	$-0.03 \pm 0.01^d$	$-1.24 \pm 0.10^d$	$16.78 \pm 0.81^c$
PLA/SeMPs-2%	$58.72 \pm 0.26^e$	$0.71 \pm 0.08^d$	$-2.67 \pm 0.05^e$	$29.71 \pm 0.81^d$

Notes: Letters of the same values are not statistically significant, according to Duncan's Multiple Range Test ( $p < 0.05$ ); a, b, and c, the means in the same column with the same letter are not significant different ( $p > 0.05$ ).

### 3.8. DPPH Free Radical Scavenging Activity

DPPH free radical scavenging activity is often used to evaluate the antioxidant activity of specific compounds or food items [40]. The higher the DPPH free radical scavenging rate, the greater the antioxidant activity. As shown in Figure 6, a significant increase was noted in the DPPH radical scavenging activity of PLA/SeMP films with SeMP concentrations of 0.5–2% ( $p < 0.05$ ), indicating that

the antioxidant property of the composite membrane was gradually enhanced. The pure PLA film does not show any antioxidant properties: thus, the antioxidant property of the composite membrane arises from SeMPs. When the concentration of SeMPs in the composite membrane was 2%, the antioxidant activity reached the maximum value of  $39.15\% \pm 0.01\%$ . This confirmed the antioxidant activity of SeMPs.

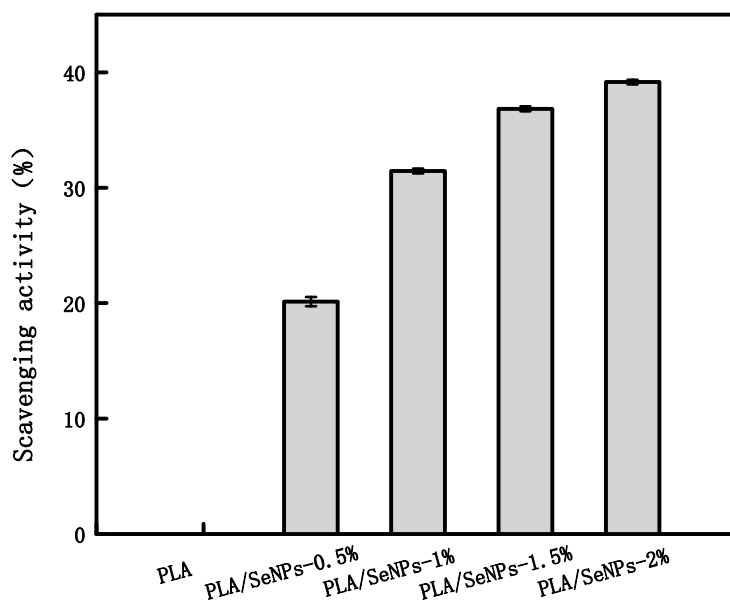


**Figure 6.** DPPH radical scavenging activities of different composite membranes. Each value represents mean  $\pm$  standard deviation (SD) of triplicates.

### 3.9. Light Transmittance

Foods spoils easily when exposed to ultraviolet light [70]. Prodpran et al. [71] found that lipid oxidation in foods could be prevented by reducing the light transmittance of the membrane. Thus, the ultraviolet light resistance is the key to food packaging membranes.

As presented in Table 4, the pure PLA was transparent, with a high transmittance value at 660 nm ( $62.51 \pm 2.58\%$ ) and a lower transmittance value at 280 nm ( $19.77 \pm 0.86\%$ ). The PLA/SeMPs films showed remarkably lower UV–vis light transmittance than that of the PLA film. When SeMPs (2%) were mixed with PLA, the light transmittance values of membranes at 280 nm decreased from  $19.77\% \pm 0.86\%$  to less than  $5.51\% \pm 0.19\%$ , which means that the nanocomposite membranes screened about 72.13% more UV light than that screened by pure PLA. The transmittance values at 660 nm decreased down to  $57.18\% \pm 1.38\%$ ,  $43.68\% \pm 1.32\%$ ,  $40.30\% \pm 0.93\%$ , and  $34.97\% \pm 0.91\%$  for PLA/0.5% SeMP, PLA/1% SeMP, PLA/1.5% SeMP, and PLA/2% SeMP nanocomposite films, respectively. This result is consistent with the physical morphology of the membrane. When the mass fraction of SeMPs was 2%, the light transmittance of the composite membrane was the lowest, reduced by 59.22% compared to that of the PLA membrane.

**Table 4.** Transmittance of different volume ratio of PLA and PLA/SeMPs films.

Sample	T <sub>660</sub> (%)	T <sub>280</sub> (%)
PLA	$62.51 \pm 2.58^a$	$19.77 \pm 0.86^a$
PLA/SeMPs-0.5%	$57.18 \pm 1.38^b$	$17.67 \pm 0.92^b$
PLA/SeMPs-1%	$43.68 \pm 1.32^c$	$7.39 \pm 0.34^c$
PLA/SeMPs-1.5%	$40.30 \pm 0.93^d$	$6.03 \pm 0.21^d$
PLA/SeMPs-2%	$34.97 \pm 0.91^e$	$5.51 \pm 0.19^d$

Notes: Letters of the same values are not statistically significant, according to Duncan's Multiple Range Test ( $p < 0.05$ ); a, b, and c, the means in the same column with the same letter are not significant different ( $p > 0.05$ ).

This indicated that the ultraviolet light barrier properties of the PLA/SeMPs membranes were much stronger than those of pure PLA. Moreover, the light transmittance of the composite films was significantly ( $p < 0.05$ ) affected by the increase in the SeMP concentration: the ultraviolet light barrier properties of the PLA/SeMPs membranes were promoted with increase in the SeMP content. The above results show that the PLA/SeMPs membranes could effectively protect food against ultraviolet light [69]. The nanocomposite films can be expected to be used as a UV screening for food packaging materials.

### 3.10. Seal Strength Determination

The seal strength is a key index used to evaluate the quality of packaging materials [57]. Due to the addition of SeMPs, the composite film, a smooth surface was formed on one side and a rough surface on the other on the smooth glass plate. After careful observation, it was determined that the side of the pure PLA film close to the glass plate was smoother than the other side, farther away from the glass plate. Figure 7 displays the sealing strengths of the pure PLA and PLA/SeMP composite membranes.

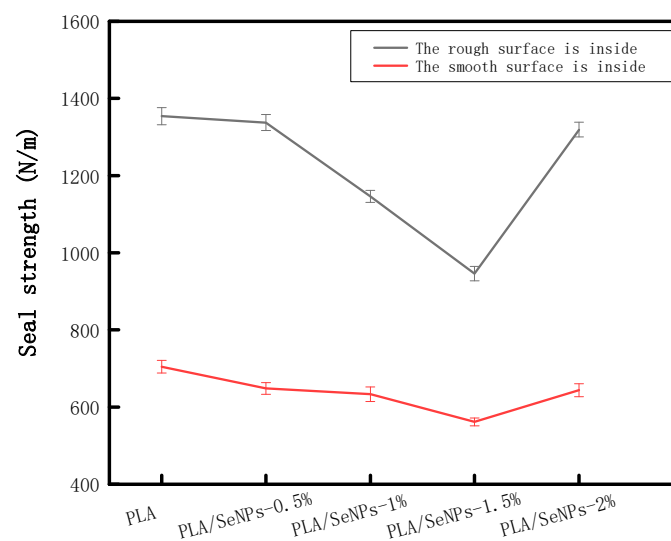


Figure 7. Seal strength of PLA and PLA/SeMPs films.

During the sealing process, the membranes are in the viscous flow state, and the high molecular weight polymer chains interpenetrate under heat and pressure [57]. Figure 7 shows that the seal strength of the rough surface was significantly higher than that of the smooth surface, irrespective of the film composition. This may be due to the uneven surface increasing the specific surface area of the film during melting, making it easier for the polymer chains to interpenetrate and intertwine and thus increasing the film's sealing performance.

Moreover, the sealing strength of the composite film decreased first and then increased with the addition of SeMPs, regardless of whether it was a rough surface or smooth surface. The sealing strength was the lowest when the mass fraction of SeMPs was 1.5%: it reached values of  $945.60 \pm 18.62$  N/m and  $561.60 \pm 10.05$  N/m for the rough surface and smooth surface, respectively, and then began to increase.

The decrease in the sealing strength may be due to the fact that the SeMPs particles were placed in the gap between PLA molecules after addition, thus blocking the interpenetration and intertwining of the high-molecular-weight polymer chains under heat and pressure [40,57]. The re-increase in the sealing strength was due to the agglomeration of SeMPs.

Although the addition of SeMPs resulted in an overall decrease in the sealing strength of the membranes, they still meet the food safety packaging requirements [72,73].

### 3.11. Antimicrobial Properties

Although SeMPs are not considered to be powerful antibiotics, an increase in scientific interest in this subject has been noted in the past few years [48]. One of the important reasons for this growing interest is the finding that elemental nano-Se has the lower toxicity compared to Se compounds and that this microelement is often found in our bodies and is important for our health compared to other popular antimicrobial agents, such as Ag. Although the exact mechanism of SeMPs' antibacterial action has not been fully elucidated, a number of possible mechanisms have been proposed. Induction of reactive oxygen species and oxidative stress are the main mechanisms that have been posited. Another possible mechanism leading to antimicrobial activity is attributable to the smaller sizes of SeMPs, which can spread through the bacterial membrane [74]. It could also be that the bactericidal mechanisms of SeMPs in PLA/SeMPs membranes are different.

The antibacterial activity of the prepared composite membranes with different concentrations of SeMPs were determined against *S. aureus* (Gram-positive) and *E. coli* (Gram-negative bacteria) via the agar disc diffusion assay (Table 5). The potential inhibitory effect of PLA membranes (without SeMPs) was used as a control to investigate. As expected, the PLA membrane showed no antimicrobial activity against *E. coli* and *S. aureus*. The antibacterial activity of PLA/SeMP membranes showed significant inhibitory effect on *E. coli* and *S. aureus*. The antibacterial activities of the membranes were thus revealed to be directly related to the SeMP content.

**Table 5.** Effect of PLA and the PLA/SeMPs composite membrane on the growth inhibition rate (%) of *E. coli* and *S. aureus* cultured at 37 °C for 24 h.

Sample	Inhibition Zone Diameter (mm)	
	<i>E. coli</i> (–)	<i>S. aureus</i> (+)
PLA	0	0
PLA/SeMPs-0.5%	12.54 ± 0.03 <sup>a</sup>	12.30 ± 0.08 <sup>a</sup>
PLA/SeMPs-1%	12.92 ± 0.05 <sup>b</sup>	12.68 ± 0.05 <sup>b</sup>
PLA/SeMPs-1.5%	13.48 ± 0.11 <sup>c</sup>	13.17 ± 0.07 <sup>c</sup>
PLA/SeMPs-2%	13.65 ± 0.06 <sup>d</sup>	13.53 ± 0.03 <sup>d</sup>

Values are presented as mean ± standard deviation. Different letters in the same column indicate significant differences ( $p < 0.05$ ).

The bacteriostatic halo of the PLA/SeMP membrane was significantly higher for Gram-negative bacteria (*E. coli*) than for the Gram-positive bacteria (*S. aureus*), indicating that Gram-negative bacteria (*E. coli*) were more susceptible to the PLA/SeMP antimicrobial membranes. However, with the increased SeMPs concentration, the inhibition zone diameters of all tested bacterial strains increased significantly. This indicates that the higher the concentration of SeMPs is, the better the antibacterial performance of the composite membrane. In addition, the PLA/2% SeMP membranes showed the largest inhibition zone against *E. coli* (13.65 ± 0.06 mm). Jamróz et al. [49] prepared binary-blend membranes of furcellaran and gelatin (FUR/GEL) and FUR/GEL composite membranes reinforced with SeMPs by solution casting. The effect of SeMPs on the antimicrobial activity of the composite membrane was also studied and a similar conclusion was obtained.

The results show that the main antibacterial component of PLA/SeMP composite membranes was SeMP, and the antibacterial ability of the PLA/SeMP composite membranes was better toward *E. coli* than against *S. aureus*. This is the first study to analyze the antibacterial activity of PLA membranes incorporated with SeMP. However, the release of SeMPs from PVA/SeMP membranes and the antibacterial mechanism of SeMPs in PLA membrane should be investigated in a future study.

## 4. Conclusions

A successful preparation of PLA/SeMP packaging materials was done in this study by the film-casting method. The effects of SeMPs on the properties of the PLA membranes were studied. FT-IR

analysis showed that SeMPs were physically trapped within the polymer matrix, and no chemical bond formation was found in the PLA and SeMPs. Although the addition of SeMPs reduced the TS and %E for these membranes in the early stages, it could improve the water resistance, ultraviolet resistance, and antibacterial and oxidation resistance of the material. The optimal composition of PVA/1.5% SeMPs had a significant antibacterial ability on *E. coli* and *S. aureus*. Overall, it is feasible to use SeMPs to enhance PLA material, the properties of which were proved. As far as the indicators studied, the properties of PLA/SeMP materials have great application potential and value in the field of food packaging, and it possess great properties for the preparation of food packaging using the SeMPs material. As for the practical value of this material in food packaging, further experiments are needed to verify it. For example, continued investigations are required to research the antifungal activities of these membranes and to evaluate the possible interactions between the food products and packaging membranes. The safety associated with the use of metal nanocomposite membrane materials in food packaging has been a matter of continued concern, owing to queries such as whether the metal nanoparticles in the composite membranes will migrate into the food and whether the migration amount will be within a safe range. These questions need to be resolved by subsequent studies. Finally, further experiments are needed to confirm whether the decline in the mechanical properties of the composite membrane is related to the particle size of the SeMPs added.

**Author Contributions:** R.L. performed the experiments and wrote the manuscript, D.E.S. prepared the manuscript, W.Q. contributed to review, D.W. edit the manuscript, J.D. project administration, S.L. developed the protocol, Y.L. is the guarantor. All authors have read and agreed to the published version of the manuscript.

**Funding:** This work was supported by Sichuan Science and Technology Program (2018RZ0034), China Scholarship Council Project (201806915013), and Natural Science Fund of Education Department of Sichuan Province (16ZB0044 and 035Z1373).

**Conflicts of Interest:** The authors declare no conflict of interest.

## References

1. Duncan, T.V. Applications of nanotechnology in food packaging and food safety: Barrier materials, antimicrobials and sensors. *J. Colloid Interface Sci.* **2011**, *363*, 1–24. [[CrossRef](#)] [[PubMed](#)]
2. Rhim, J.W.; Park, H.M.; Ha, C.S. Bio-nanocomposites for food packaging applications. *Prog. Polym. Sci.* **2013**, *38*, 1629–1652. [[CrossRef](#)]
3. Yusoff, R.B.; Takagi, H.; Nakagaito, A.N. Tensile and flexural properties of polylactic acid-based hybrid green composites reinforced by kenaf, bamboo and coir fibers. *Ind. Crops Prod.* **2016**, *94*, 562–573. [[CrossRef](#)]
4. Norma, M.; Thanh, P.; Maria-Beatrice, C.; Patrizia, C.; Andrea, L. Poly(lactic acid) (PLA) based tear resistant and biodegradable flexible films by blown film extrusion. *Materials* **2018**, *11*, 148–162. [[CrossRef](#)]
5. Agarwal, M.; Koelling, K.W.; Chalmers, J.J. Characterization of the degradation of polylactic acid polymer in a solid substrate environment. *Biotechnol. Prog.* **1998**, *14*, 517–526. [[CrossRef](#)] [[PubMed](#)]
6. Drumright, R.E.; Gruber, P.R.; Henton, D.E. Polylactic acid technology. *Adv. Mater.* **2000**, *12*, 1841–1846. [[CrossRef](#)]
7. Garlotta, D. A literature review of poly(lactic acid). *J. Polym. Environ.* **2001**, *9*, 63–84. [[CrossRef](#)]
8. Eslami, H.; Kamal, M.R. Elongational rheology of biodegradable poly(lactic acid)/poly[(butylene succinate)-co-adipate] binary blends and poly(lactic acid)/poly[(butylene succinate)-co-adipate]/clay ternary nanocomposites (pages 2290–2306). *J. Appl. Polym. Sci.* **2014**, *127*, 2290–2306. [[CrossRef](#)]
9. Tawakkal, I.S.M.A.; Cran, M.J.; Miltz, J.; Bigger, S.W. A review of poly(lactic acid)-based materials for antimicrobial packaging. *J. Food Sci.* **2014**, *79*, R1477–R1490. [[CrossRef](#)]
10. Zhu, J.Y.; Tang, C.H.; Yin, S.W.; Yang, X.Q. Development and characterization of novel antimicrobial bilayer films based on polylactic acid (PLA)/pickering emulsions. *Carbohydr. Polym.* **2018**, *181*, 727–735. [[CrossRef](#)]
11. Gordobil, O.; Delucis, R.; Egüés, I.; Labidia, J. Kraft lignin as filler in PLA to improve ductility and thermal properties. *Ind. Crops Prod.* **2015**, *72*, 46–53. [[CrossRef](#)]
12. Appendini, P.; Hotchkiss, J.H. Review of antimicrobial food packaging. *Innov. Food Sci. Emerg. Technol.* **2002**, *3*, 113–126. [[CrossRef](#)]

13. Therias, S.; Larché, J.-F.; Bussi re, P.-O.; Gardette, J.L.; Dubois, P. Photochemical behavior of polylactide/ZnO nanocomposite films. *Biomacromolecules* **2012**, *13*, 3283–3291. [[CrossRef](#)] [[PubMed](#)]
14. Fortunati, E.; Rinaldi, S.; Peltzer, M.; Bloise, N.; Visai, L.; Armentano, I.; Kenny, M. Nano-biocomposite films with modified cellulose nanocrystals and synthesized silver nanoparticles. *Carbohydr. Polym.* **2014**, *101*, 1122–1133. [[CrossRef](#)]
15. Luo, Z.; Qin, Y.; Ye, Q. Effect of nano-TiO<sub>2</sub>-ldpe packaging on microbiological and physicochemical quality of pacific white shrimp during chilled storage. *Int. J. Food Sci. Technol.* **2015**, *50*, 1567–1573. [[CrossRef](#)]
16. Silveira, A.C.; Moreira, G.C.; Art s, F.; Aguayo, E. Vanillin and cinnamic acid in aqueous solutions or in active modified packaging preserve the quality of fresh-cut cantaloupe melon. *Sci. Hortic.* **2015**, *192*, 271–278. [[CrossRef](#)]
17. Athanasouliaa, I.G.; Mikropouloua, M.; Karapati, S.; Tarantili, P.; Trapalis, C. Study of thermomechanical and antibacterial properties of TiO<sub>2</sub>/Poly(lactic acid) nanocomposites. *Mater. Today Proceed.* **2018**, *5*, 27553–27562. [[CrossRef](#)]
18. Shebi, A.; Lisa, S. Evaluation of biocompatibility and bactericidal activity of hierarchically porous PLA-TiO<sub>2</sub> nanocomposite films fabricated by breath-figure method. *Mater. Chem. Phys.* **2019**, *230*, 308–318. [[CrossRef](#)]
19. Munteanu, B.S.; Aytac, Z.; Pricope, G.M.; Uyar, T.; Vasile, C. Polylactic acid (PLA)/Silver-NP/Vitamin E bionanocomposite electrospun nanofibers with antibacterial and antioxidant activity. *J. Nanopart. Res.* **2014**, *16*, 2643. [[CrossRef](#)]
20. Shameli, K.; Ahmad, M.B.; Yunus, W.M.Z.W.; Ibrahim, N.A.; Rahman, R.A.; Jokar, M.; Darroudi, M. Silver/poly (lactic acid) nanocomposites: Preparation, characterization, and antibacterial activity. *Int. J. Nanomed.* **2010**, *5*, 573–579. [[CrossRef](#)]
21. Cremonini, E.; Zonaro, E.; Donini, M.; Lampis, S.; Boaretti, M.; Dusi, S.; Vallini, G. Biogenic selenium nanoparticles: Characterization, antimicrobial activity and effects on human dendritic cells and fibroblasts. *Microb. Biotechnol.* **2016**, *9*, 758–771. [[CrossRef](#)] [[PubMed](#)]
22. Shoeibi, S.; Mashreghi, M. Biosynthesis of selenium nanoparticles using *Enterococcus faecalis* and evaluation of their antibacterial activities. *J. Trace Elem. Med. Biol.* **2017**, *39*, 135–139. [[CrossRef](#)] [[PubMed](#)]
23. Tran, P.A.; O’Brien-Simpson, N.; Reynolds, E.C.; Pantarat, N.; Biswas, D.P.; O’Connor, A.J. Low cytotoxic trace element selenium nanoparticles and their differential antimicrobial properties against *S. aureus* and *E. coli*. *Nanotechnology* **2015**, *27*, 045101. [[CrossRef](#)] [[PubMed](#)]
24. Guisbiers, G.; Wang, Q.; Khachatryan, E.; Mimun, L.C.; Mendoza-Cruz, R.; Larese-Casanova, P.; Nash, K.L. Inhibition of *E. coli* and *S. aureus* with selenium nanoparticles synthesized by pulsed laser ablation in deionized water. *Int. J. Nanomed.* **2016**, *11*, 3731–3736. [[CrossRef](#)]
25. Redman, C.; Scott, J.A.; Baines, A.T.; Basye, J.L.; Clark, L.C.; Calleye, C.; Nelson, M.A. Inhibitory effect of selenomethionine on the growth of three selected human tumor cell lines. *Cancer Lett.* **1998**, *125*, 103–110. [[CrossRef](#)]
26. Roman, M.; Jitaru, P.; Barbante, C. Selenium biochemistry and its role for human health. *Metallomics* **2013**, *6*, 25–54. [[CrossRef](#)]
27. Kalishwaralal, K.; Jeyabharathi, S.; Sundar, K.; Muthukumaran, A. Comparative analysis of cardiovascular effects of selenium nanoparticles and sodium selenite in zebrafish embryos. *Artif. Cells Nanomed. Biotechnol.* **2015**, *44*, 1–7. [[CrossRef](#)]
28. Kalishwaralal, K.; Jeyabharathi, S.; Sundar, K.; Muthukumaran, A. A novel one-pot green synthesis of selenium nanoparticles and evaluation of its toxicity in zebrafish embryos. *Artif. Cells Nanomed. Biotechnol.* **2014**, *44*, 1–7. [[CrossRef](#)]
29. Weekley, C.M.; Harris, H.H. Which form is that? the importance of selenium speciation and metabolism in the prevention and treatment of disease. *Chem. Soc. Rev.* **2013**, *42*, 8870–8910. [[CrossRef](#)]
30. Huawei, Z.; Jay, C.; Gerald, C. Selenium in bone health: Roles in antioxidant protection and cell proliferation. *Nutrients* **2013**, *5*, 97–110. [[CrossRef](#)]
31. Moreno-Reyes, R.; Egrise, D.; Neve, J.; Pasteels, J.L.; Schoutens, A. Selenium deficiency-induced growth retardation is associated with an impaired bone metabolism and osteopenia. *J. Bone Miner. Res.* **2001**, *16*, 1556–1563. [[CrossRef](#)] [[PubMed](#)]
32. Cao, J.J.; Gregoire, B.R.; Zeng, H. Selenium deficiency decreases antioxidative capacity and is detrimental to bone microarchitecture in mice. *J. Nutr.* **2012**, *142*, 1526–1531. [[CrossRef](#)] [[PubMed](#)]

33. Vinceti, M.; Mandrioli, J.; Borella, P.; Michalke, B.; Tsatsakis, A.; Finkelstein, Y. Selenium neurotoxicity in humans: Bridging laboratory and epidemiologic studies. *Toxicol. Lett.* **2014**, *230*, 295–303. [[CrossRef](#)] [[PubMed](#)]
34. Morris, J.; Crane, S. Selenium toxicity from a misformulated dietary supplement, adverse health effects, and the temporal response in the nail biologic monitor. *Nutrients* **2013**, *5*, 1024–1057. [[CrossRef](#)] [[PubMed](#)]
35. Wang, H.; Zhang, J.; Yu, H. Elemental selenium at nano size possesses lower toxicity without compromising the fundamental effect on selenoenzymes: Comparison with selenomethionine in mice. *Free Radic. Biol. Med.* **2007**, *42*, 1524–1533. [[CrossRef](#)] [[PubMed](#)]
36. Zhang, J.S.; Gao, X.Y.; Zhang, L.D.; Bao, Y.P. Biological effects of a nano red elemental selenium. *Biofactors* **2001**, *15*, 27–38. [[CrossRef](#)]
37. Hoffmann, P.R.; Berry, M.J. The influence of selenium on immune responses. *Mol. Nutr. Food Res.* **2008**, *52*, 1273–1280. [[CrossRef](#)]
38. Stevanović, M.; Filipović, N.; Djurdjević, J.; Lukić, M.; Milenković, M.; Boccaccini, A. 4555Bioglass®-based scaffolds coated with selenium nanoparticles or with poly (lactide-co-glycolide)/selenium particles: Processing, evaluation and antibacterial activity. *Colloids Surf. B Biointerfaces* **2015**, *132*, 208–215. [[CrossRef](#)]
39. Sun, L.; Sun, J.; Chen, L.; Niu, P.; Yang, X.; Guo, Y. Preparation and characterization of chitosan film incorporated with thinned young apple polyphenols as an active packaging material. *Carbohydr. Polym.* **2017**, *163*, 81–91. [[CrossRef](#)]
40. Liu, Y.; Wang, S.; Lan, W.; Qin, W. Fabrication and testing of PVA/Chitosan bilayer films for strawberry packaging. *Coatings* **2017**, *7*, 109. [[CrossRef](#)]
41. Gontard, N.; Duchez, C.; CUQ, J.L.; Guilbert, S. Edible composite films of wheat gluten and lipids: water vapour permeability and other physical properties. *Int. J. Food Sci. Technol.* **1994**, *29*, 39–50. [[CrossRef](#)]
42. Fabra, M.J.; López-Rubio, A.; Lagaron, J.M. Use of the electrohydrodynamic process to develop active/bioactive bilayer films for food packaging applications. *Food Hydrocoll.* **2016**, *55*, 11–18. [[CrossRef](#)]
43. Luchese, C.L.; Uranga, J.; Spada, J.C.; Tessaro, I.C.; de la Caba, K. Valorisation of blueberry waste and use of compression to manufacture sustainable starch films with enhanced properties. *Int. J. Biol. Macromol.* **2018**, *115*, 955–960. [[CrossRef](#)] [[PubMed](#)]
44. Atoui, A.K.; Mansouri, A.; Boskou, G.; Kefalas, P.J. Tea and herbal infusions: Their antioxidant activity and phenolic profile. *Food Chem.* **2005**, *89*, 27–36. [[CrossRef](#)]
45. Yu, Z.; Alsammarrhaie, F.K.; Nayigiziki, F.X.; Wang, W.; Vardhanabhuti, B.; Mustapha, A.; Lin, M. Effect and mechanism of cellulose nanofibrils on the active functions of biopolymer-based nanocomposite films. *Food Res. Int.* **2017**, *99*, 166–172. [[CrossRef](#)] [[PubMed](#)]
46. Otoni, C.G.; de Moura, M.R.; Aouada, F.A.; Camilloto, G.P.; Cruz, R.S.; Lorevice, M.V.; Mattoso, L.H. Antimicrobial and physical-mechanical properties of pectin/papaya puree/cinnamaldehyde nanoemulsion edible composite films. *Food Hydrocoll.* **2014**, *41*, 188–194. [[CrossRef](#)]
47. Liu, X.; Chen, X.; Ren, J.; Chang, M.; He, B.; Zhang, C. Effects of nano-ZnO and nano-SiO<sub>2</sub> particles on properties of PVA/xylan composite films. *Int. J. Biol. Macromol.* **2019**, *132*, 978–986. [[CrossRef](#)]
48. Filipović, N.; Veselinović, L.; Ražić, S.; Jeremić, S.; Filipič, M.; Žegura, B.; Stevanović, M. Poly ( $\epsilon$ -caprolactone) microspheres for prolonged release of selenium nanoparticles. *Mater. Sci. Eng. C* **2019**, *96*, 776–789. [[CrossRef](#)]
49. Jamróz, E.; Kopel, P.; Juszczak, L.; Kawecka, A.; Bytesnikova, Z.; Milosavljević, V.; Adam, V. Development and characterisation of furcellaran-gelatin films containing SeNPs and AgNPs that have antimicrobial activity. *Food Hydrocoll.* **2018**, *83*, 9–16. [[CrossRef](#)]
50. Ahmed, J.; Arfat, Y.A.; Castro-Aguirre, E.; Auras, R. Mechanical, structural and thermal properties of Ag–Cu and ZnO reinforced polylactide nanocomposite films. *Int. J. Biol. Macromol.* **2016**, *86*, 885–892. [[CrossRef](#)]
51. Li, S.C.; Li, Y.N. Mechanical and antibacterial properties of modified nano-ZnO/high-density polyethylene composite films with a low doped content of nano-ZnO. *J. Appl. Polym. Sci.* **2010**, *116*, 2965–2969. [[CrossRef](#)]
52. Hosseini, S.F.; Rezaei, M.; Zandi, M.; Ghavi, F.F. Preparation and functional properties of fish gelatin–chitosan blend edible films. *Food Chem.* **2013**, *136*, 1490–1495. [[CrossRef](#)]
53. Pereda, M.; Amica, G.; Marcovich, N.E. Development and characterization of edible chitosan/olive oil emulsion films. *Carbohydr. Polym.* **2012**, *87*, 1318–1325. [[CrossRef](#)]
54. Pranoto, Y.; Salokhe, V.M.; Rakshit, S.K. Physical and antibacterial properties of alginate-based edible film incorporated with garlic oil. *Food Res. Int.* **2005**, *38*, 267–272. [[CrossRef](#)]

55. Wang, L.; Dong, Y.; Men, H.; Tong, J.; Zhou, J. Preparation and characterization of active films based on chitosan incorporated tea polyphenols. *Food Hydrocoll.* **2013**, *32*, 35–41. [[CrossRef](#)]
56. Turalija, M.; Bischof, S.; Budimir, A.; Gaan, S. Antimicrobial PLA films from environment friendly additives. *Compos. Part B Eng.* **2016**, *102*, 94–99. [[CrossRef](#)]
57. Ye, J.; Wang, S.; Lan, W.; Qin, W.; Liu, Y. Preparation and properties of polylactic acid-tea polyphenol-chitosan composite membranes. *Int. J. Biol. Macromol.* **2018**, *117*, 632–639. [[CrossRef](#)]
58. Hauri, J.F.; Niece, B.K. Leaching of silver from silver-impregnated food storage containers. *J. Chem. Educ.* **2011**, *88*, 1407–1409. [[CrossRef](#)]
59. Xia, S.; Liu, X.; Wang, J.; Kan, Z.; Chen, H.; Fu, W.; Li, Z. Role of poly (ethylene glycol) grafted silica nanoparticle shape in toughened PLA-matrix nanocomposites. *Compos. Part B Eng.* **2019**, *168*, 398–405. [[CrossRef](#)]
60. Liu, Y.; Wang, S.; Lan, W.; Qin, W. Fabrication of polylactic acid/carbon nanotubes/chitosan composite fibers by electrospinning for strawberry preservation. *Int. J. Biol. Macromol.* **2019**, *121*, 1329–1336. [[CrossRef](#)]
61. Yoshida, C.M.; Maciel, V.B.V.; Mendonça, M.E.D.; Franco, T.T. Chitosan biobased and intelligent films: Monitoring pH variations. *LWT Food Sci. Technol.* **2014**, *55*, 83–89. [[CrossRef](#)]
62. Gutiérrez, T.J.; Tapia, M.S.; Pérez, E.; Famá, L. Structural and mechanical properties of edible films made from native and modified cush-cush yam and cassava starch. *Food Hydrocoll.* **2015**, *45*, 211–217. [[CrossRef](#)]
63. Shankar, S.; Wang, L.F.; Rhim, J.W. Incorporation of zinc oxide nanoparticles improved the mechanical, water vapor barrier, UV-light barrier, and antibacterial properties of PLA-based nanocomposite films. *Mater. Sci. Eng. C* **2018**, *93*, 289–298. [[CrossRef](#)]
64. Fan, C.; Chi, H.; Zhang, C.; Cui, R.; Lu, W.; Yuan, M.; Qin, Y. Effect of multiscale structure on the gas barrier properties of poly (lactic acid)/Ag nanocomposite films. *Polym. Adv. Technol.* **2019**, *30*, 1709–1715. [[CrossRef](#)]
65. Shankar, S.; Rhim, J.W.; Won, K. Preparation of poly (lactide)/lignin/silver nanoparticles composite films with UV light barrier and antibacterial properties. *Int. J. Biol. Macromol.* **2018**, *107*, 1724–1731. [[CrossRef](#)]
66. Jeon, I.Y.; Baek, J.B. Nanocomposites derived from polymers and inorganic nanoparticles. *Materials* **2010**, *3*, 3654–3674. [[CrossRef](#)]
67. Garrido, T.; Etxabide, A.; Peñalba, M.; De La Caba, K.; Guerrero, P. Preparation and characterization of soy protein thin films: Processing–properties correlation. *Mater. Lett.* **2013**, *105*, 110–112. [[CrossRef](#)]
68. Ramos, Ó.L.; Reinas, I.; Silva, S.I.; Fernandes, J.C.; Cerqueira, M.A.; Pereira, R.N.; Malcata, F.X. Effect of whey protein purity and glycerol content upon physical properties of edible films manufactured therefrom. *Food Hydrocoll.* **2013**, *30*, 110–122. [[CrossRef](#)]
69. Wang, X.; Yong, H.; Gao, L.; Li, L.; Jin, M.; Liu, J. Preparation and characterization of antioxidant and pH-sensitive films based on chitosan and black soybean seed coat extract. *Food Hydrocoll.* **2019**, *89*, 56–66. [[CrossRef](#)]
70. Martins, J.T.; Cerqueira, M.A.; Vicente, A.A. Influence of  $\alpha$ -tocopherol on physicochemical properties of chitosan-based films. *Food Hydrocoll.* **2012**, *27*, 220–227. [[CrossRef](#)]
71. Prodpran, T.; Benjakul, S.; Phatcharat, S. Effect of phenolic compounds on protein cross-linking and properties of film from fish myofibrillar protein. *Int. J. Biol. Macromol.* **2012**, *51*, 774–782. [[CrossRef](#)]
72. Tongnuanchan, P.; Benjakul, S.; Prodpran, T.; Pisuchpen, S.; Osako, K. Mechanical, thermal and heat sealing properties of fish skin gelatin film containing palm oil and basil essential oil with different surfactants. *Food Hydrocoll.* **2016**, *56*, 93–107. [[CrossRef](#)]
73. Farhan, A.; Hani, N.M. Characterization of edible packaging films based on semi-refined kappa-carrageenan plasticized with glycerol and sorbitol. *Food Hydrocoll.* **2017**, *64*, 48–58. [[CrossRef](#)]
74. Hajji, S.; Salem, R.B.S.B.; Hamdi, M.; Jellouli, K.; Ayadi, W.; Nasri, M.; Boufi, S. Nanocomposite films based on chitosan–poly (vinyl alcohol) and silver nanoparticles with high antibacterial and antioxidant activities. *Process Saf. Environ. Prot.* **2017**, *111*, 112–121. [[CrossRef](#)]

